X-625-71-459

PREPRINT

NASA TM X- 65773

ION CLUSTERS AND THE VENUS ULTRAVIOLET HAZE LAYER

A. C. AIKIN

NOVEMBER 1971

GSFC

GODDARD SPACE FLIGHT CENTER
GREENBELT, MARYLAND

N72-12842 (NASA-TM-X-65773) ION CLUSTERS AND THE VENUS ULTRAVIOLET HAZE LAYER A.C. Aikin (NASA) Nov. 1971 8 p CSCL 03B

Unclas 09753 G3/30

FACILITY

11TX 65773 (NASA CR OR TMX OR AD NUMBER) 30 (CATEGORY)

ION CLUSTERS AND THE VENUS ULTRAVIOLET HAZE LAYER

by

A. C. Aikin
Laboratory for Planetary Atmospheres
NASA/Goddard Space Flight Center
Greenbelt, Maryland

The daytime ionosphere of Venus is observed between 100 and 500 km altitude with a peak electron concentration of 5×10^{5} cm^{-3} at 140 km.[1] Below 200 km CO_2^+ is thought to be the principal ion[2, 3] unless oxygen is present. We suggest that at altitudes less than 130 km the ion $CO_2^+ \cdot CO_2$ is an important ionic constituent of the Venus ionosphere. Below 100 km ion clustering processes combine with the low temperature at the mesopause to form coagulates giving rise to the ultraviolet haze layer which has frequently been observed.

For clustering of neutrals to ions Keller and Beyer[4] have shown the dependence of clustering rate on the polarizability of the neutral molecule and the mass of the ion. A rate of $k_1 = 5 \times 10^{-30} cm^6 sec^{-1}$ and $k_{-1} = 5 \times 10^{-14} cm^3 sec^{-1}$ would be predicted for the reactions

$$CO_2^+ + CO_2 + CO_2 \underset{k_{-1}}{\overset{k_1}{\rightleftarrows}} CO_2^+ \cdot CO_2 + CO_2 \qquad (1)$$

The forward reaction has been observed in the laboratory with a rate of 3×10^{-28} cm^6 sec^{-1} at 1 ev[5]. In addition dissociative ion-electron recombination is operative in the ionosphere

$$CO_2^+ \cdot CO_2 + e \rightarrow CO_2 + CO_2 \qquad (2)$$

Based on a measured rate of 2.3×10^{-6} cm^3 sec^{-1} for O_4^+ - electron recombination[6] a rate of $\alpha_D = 2.3 \times 10^{-6} (\frac{300}{T})$ will be assumed for (2) where T is the temperature. The ratio $CO_2^+ \cdot CO_2/CO_2^+$ is

$$\frac{[CO_2^+ \cdot CO_2]}{[CO_2^+]} = \frac{k_1 [CO_2]^2}{k_{-1}[CO_2] + \alpha_D N_e} \qquad (3)$$

and plotted as a function of altitude in Figure 1. The atmospheric model chosen is the Goddard Space Flight Center model[7]. At altitudes below 90 km, where cosmic rays are the dominant source of ionization the ion ratio

$$\frac{[CO_2^+ \cdot CO_2]}{[CO_2^+]}$$

is greater than one. Above 100 km the ratio is less than unity.

If N_2 and O_2 are present in the Venus atmosphere, then the processes

$$CO_2^+ + N_2 + CO_2 \rightarrow CO_2^+ \cdot N_2 + CO_2 \qquad (4)$$

and

$$CO_2^+ + O_2 + CO_2 \rightarrow CO_2^+ \cdot O_2 + CO_2 \qquad (5)$$

as well as $CO_2^+ + O_2 \rightarrow O_2^+ + CO_2$ will cause loss of CO_2^+. The formation and loss processes of $O_2^+ \cdot CO_2$ have been discussed previously for the case of the Martian atmosphere[8].

The presence of O_2 will lead to the formation of negative ions[9] which will modity (3) by the addition of a loss term for $CO_2^+ \cdot CO_2$ involving ion-ion recombination.

In the event that water vapor is present above the cloud tops reaction occur such as

$$CO_2^+ \cdot CO_2 + H_2O + CO_2 \rightarrow CO_2^+ \cdot H_2O + CO_2 \qquad (6)$$

$$CO_2^+ \cdot H_2O + H_2O \rightarrow H_3O^+ + CO_2 + OH \qquad (7)$$

Coffey[10] has shown that $H_3O^+ \cdot (H_2O)_n$ can react with NH_4 and HCl to form $NH_4Cl \cdot (H_2O)_n$ by the chain

$$H_3O^+ \cdot (H_2O)_n + NH_4 \rightarrow NH_4^+ \cdot (H_2O)_n + H_3O \qquad (8)$$

$$NH_4^+ \cdot (H_2O)_n + HCl \rightarrow NH_4Cl(H_2O)_m + H_3^+O(H_2O)_{(n-m)} \qquad (9)$$

It has further been observed that the compound $NH_4Cl(H_2O)_m$ coagulates easily to form micron sized particles.

Kuiper[11] has suggested that the Venus ultraviolet haze layer is composed of 0.1μ sized particles of NH_4Cl. The location of this layer at 90 km is illustrated in

Figure 2 which shows the temperature distribution for the atmospheric model employed. Also indicated are the levels of the yellow haze layer and the ratio of cluster ions relative to CO_2^+.

An alternate source of coagulates may be the ion $CO_2^+ \cdot H_2O$, which can attach additional water molecules as well as other neutral molecules. The complexes $CO_2^+ \cdot (H_2O) \cdot XY$ can form as has been observed with NO^+, H_2O, SO_2 systems[12]. The resulting complex will further react to eliminate the ion and form coagulatable compounds. Laboratory studies at Venus atmosphere conditions will define more clearly the importance of ion clustering processes in the formation of the Venus ultraviolet haze layer.

REFERENCES

1. Fjeldbo, G. and V.R. Eshleman, Radio Science, 4, 879, (1969).
2. McElroy, M.B., J. Geophys. Res., 74, 29 (1969).
3. Herman, J.R., R.E. Hartle and S.J. Bauer, Planet. Space Sci., 19, 443 (1971).
4. Beyer, R.A. and G.E. Keller, Trans. Am. Geophys. Union, 52, 303 (1970).
5. Paulson, J.F., F. Dale and R.L. Mosher, Nature, 204, 377 (1964).
6. Kasner, W.H. and M.A. Biondi, Phys. Rev., 174, 139 (1968).
7. Ainsworth, J.E., Goddard Space Flight Center Document, X-625-70-203 (1970).
8. Whitten, R.C., I.G. Poppoff and J.S. Sims, Planet. Space Sci., 19, 243 (1971).
9. Aikin, A.C., Icarus, 9, 487 (1968).
10. Coffey, P.C., Bull. Am. Phys. Soc., 16, (1971).
11. Kuiper, G., Comm. of the Lunar and Planet. Lab. Comm. NOS 100-104, 6, 229 University of Arizona 1968-1969.
12. Castleman, A.W., I.N. Tang and H.R. Munkelwitz, Science, 173, 1025 (1971).

FIGURE CAPTIONS

Figure 1 - The ratio $CO_2^+ \cdot CO_2/CO_2^+$ as a function of altitude.

Figure 2 - Altitude level of the Venus yellow cloud layer and untraviolet haze layer in relation to the temperature distribution of the atmosphere and the ratio of $CO_2^+ \cdot CO_2$ to CO_2^+.

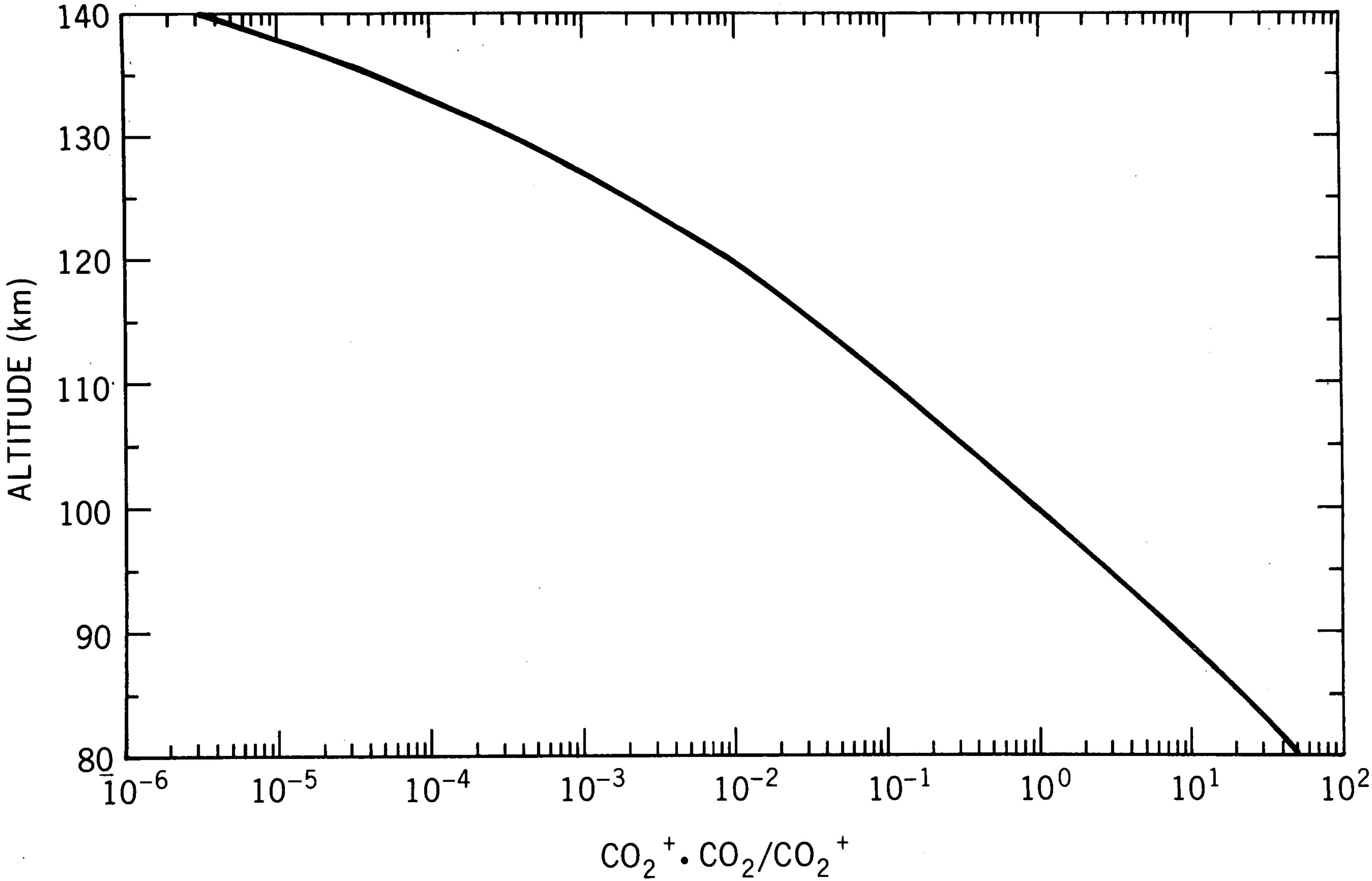

140
130
120
110
100
90
80
ALTITUDE (km)
10^{-6}
10^{-5}
10^{-4}
10^{-3}
10^{-2}
10^{-1}
10^{0}
10^{1}
10^{2}
$CO_2^+ \cdot CO_2/CO_2^+$

Figure 1

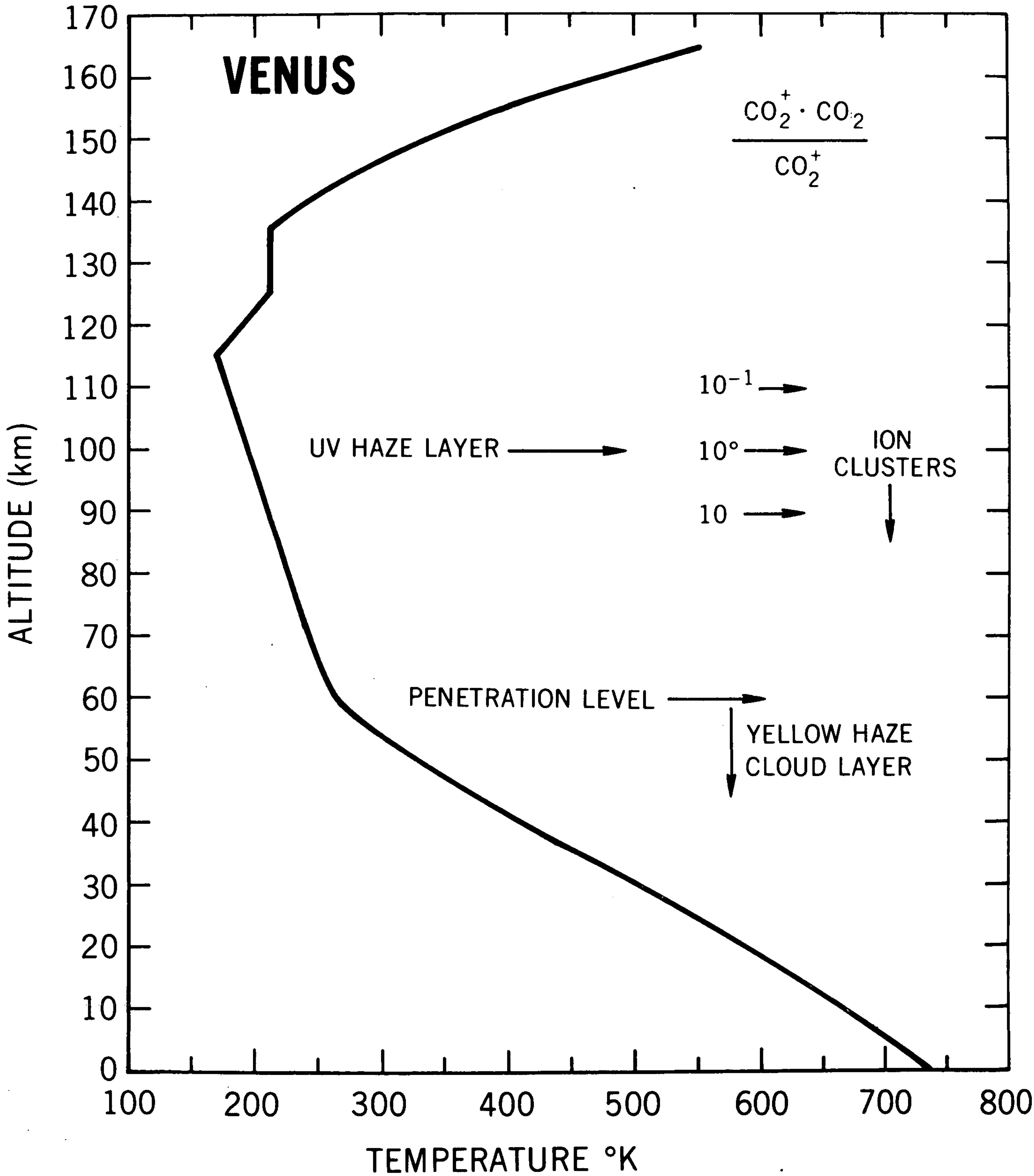
VENUS
$\frac{CO_2^+ \cdot CO_2}{CO_2^+}$
10^{-1}
UV HAZE LAYER
10°
ION CLUSTERS
10
PENETRATION LEVEL
YELLOW HAZE CLOUD LAYER
ALTITUDE (km)
TEMPERATURE °K
170
160
150
140
130
120
110
100
90
80
70
60
50
40
30
20
10
0
100
200
300
400
500
600
700
800

Figure 2